J Therm Anal Calorim (2012) 107:1167–1176
DOI 10.1007/s10973-011-1368-1

Kinetics and mechanism of degradation of Co(II)–*N*-benzyloxycarbonylglycinato complex

Dragica M. Minić · Maja T. Šumar-Ristović · Đenana U. Miodragović · Katarina K. Anđelković · Dejan Poleti

Received: 29 November 2010 / Accepted: 20 January 2011 / Published online: 12 February 2011

Abstract The kinetics of multi-step thermal degradation of Co(II) complex with *N*-benzyloxycarbonyl glycinato ligand $[Co(N\text{-Boc-gly})_2(H_2O)_4]\cdot 2H_2O$, in non-isothermal conditions was studied using isoconversional and non-isoconversional methods. The degradation of complex occurs in three well-separated steps involving the loss of water molecules in first step followed by two degradation steps of dehydrated complex. The dependence of Arrhenius parameters on conversion degree showed that all observed steps of thermal degradation are very complex, involving more than one elementary step, as can be expected for most solid-state heterogeneous reactions with solid reactants and solid and gaseous products. It was shown that step 1, corresponding to the dehydration, involves a series of competitive dehydration steps of differently bound water molecules complicated by diffusion. Second step involves two parallel reactions related to the loss of two identical $C_6H_5CH_2O$– ligand fragments complicated by the presence of products in gaseous state. Further degradation in step 3 corresponds to complex process with a change in the limiting stage, in this case from the kinetic to the diffusion regime, connected with the presence of gaseous products diffusing through the solid product.

Keywords Co–*N*-benzyloxycarbonylglycinato complex · Activation energy · Dehydration · Degradation · Kinetics

Introduction

Very interesting structural and biological properties of *N*-substituted amino acids as ligands [1–14] generated our interest for *N*-benzyloxycarbonyl-protected amino acids and their transition metal complexes [15–17]. *N*-benzyloxycarbonyl-protected amino acids and their derivatives have been reported to act as anti-convulsing, anti-inflammatory and anti-neoplastic agents [7–9]. It was found that *N*-benzyloxycarbonylglycinato ligand, *N*-Boc-gly, exhibits better anti-convulsing activity than glycine itself [10]. Besides biological, we also found antimicrobial and antifungal activities of this ligand and its complexes with Co(II), Cd(II) and Zn(II) [16]. It was shown that the complexes exhibit the best inhibitory activity against *Candida albicans*.

In our previous study on thermal stability of transition metal *N*-Boc-gly complexes [17] it was shown that the mechanism of multi-step thermal degradation starts with a loss of water molecules from the outer sphere of the complexes. This process is followed immediately by removal of water molecules from the inner sphere of the complexes, yielding stable anhydrous intermediate. At higher temperatures, this intermediate undergoes further degradation involving ligand fragmentation, which occurs in two steps. The enthalpies and kinetic parameters of the degradation processes: the pre-exponential factor, Z, and the apparent activation energy, E_a, for each step of

D. M. Minić (✉)
Faculty of Physical Chemistry, University of Belgrade, Studentski trg 16, 11000 Belgrade, Serbia
e-mail: dminic@ffh.bg.ac.rs

M. T. Šumar-Ristović · Đ. U. Miodragović · K. K. Anđelković
Faculty of Chemistry, University of Belgrade, Studentski trg 16, 11000 Belgrade, Serbia

D. Poleti
Faculty of Technology and Metallurgy, University of Belgrade, Karnegijeva 4, 11000 Belgrade, Serbia

degradation, were determined by Kissinger's, Ozawa's and Friedman's isoconversion methods [17]. However, the kinetics and mechanism of each step were not analyzed in detail. With this in mind, we present a comprehensive kinetic study of degradation of the $[Co(N\text{-Boc-gly})_2(H_2O)_4]\cdot 2H_2O$ complex allowing high reliability determination of kinetic parameters and deeper insight into reaction mechanism.

There are many papers describing thermal stability of transition metal complexes together with their characterization, physical properties and structural features [18–23]. However, studies on the basic kinetic analysis of TG and DTG/DSC data of these systems are quite scarce, offering no more than kinetic parameters, Z and E_a [24–29], or kinetic triplets [30]. In addition, most papers treating degradation of complex compounds did not follow the criteria suggested for finding the true kinetic parameters [31–34]. Since these criteria were established mainly for thermal and thermo-oxidative degradation of polymers and polymeric materials, the investigation presented here could be regarded as a case study using a transition metal complex instead of polymeric materials.

Experimental

The Co(II) complex with the *N*-Boc-gly ligand $[Co(N\text{-Boc-gly})_2(H_2O)_4]\cdot 2H_2O$ was prepared in a simple ligand exchange reaction between $CoCl_2\cdot 6H_2O$ and *N*-Boc-glyH (molar ratio 1:2, ethanol–water mixture, pH = 5–6), as described earlier [15].

The process of thermal degradation of Co-complex was studied non-isothermally by using a SDT Q600 (TA Instruments) apparatus for simultaneous TG-DTA analysis.

TG experiments at different heating rates (5–20 °C min^{-1}) were performed from room temperature to 650 °C with sample mass of about 6 mg in a dry nitrogen atmosphere (flow rate 100 cm^3 min^{-1}) using Pt crucibles and the Pt crucibles with Al_2O_3 as reference material. DTA curve was recorded simultaneously with TG data.

Methodological aspects of solid-state kinetics in non-isothermal conditions

Thermal analysis methods are very useful tools for kinetic analysis of the solid-state reactions of different compounds. In calorimetric measurements the solid-state reaction involving heating of the sample can be performed in several ways using isothermal as well as non-isothermal methods. Non-isothermal experiments are more convenient to perform than isothermal ones. Mathematical description of these reactions usually includes a kinetic triplet involving Arrhenius parameters (an activation energy, E and a pre-exponential factor, Z) as well as an algebraic expression of the conversion function, $f(\alpha)$, which describes the dependence of the reaction rate on the conversion degree, α.

The conversion degree, α, is related to the experimental data as follows [35]:

$$\frac{d\alpha}{dt} = Z\exp\left(-\frac{E}{RT}\right)f(\alpha) \tag{1}$$

where R is the gas constant, t is time and T is absolute temperature.

It is obvious that the constant value of the activation energy can be expected only for a single-step reaction and E in Eq. 1 becomes an apparent quantity (an apparent activation energy, E_a) based on a quasi single-step reaction.

For non-isothermal measurements at a constant heating rate $\beta = dT/dt$, Eq. 1 is transformed to:

$$\beta\frac{d\alpha}{dT} = Z\exp\left(-\frac{E_a}{RT}\right)f(\alpha). \tag{2}$$

The integral form of the conversion function, $g(\alpha)$, can be obtained by applying the integration on the Eq. 2 and by separating the variables:

$$g(\alpha) = \int_0^{\alpha}\frac{d\alpha}{f(\alpha)} = \frac{ZE_a}{R\beta}p(x) \tag{3}$$

where $p(x)$ is the temperature integral:

$$p(x) = \int_0^{x}\frac{\exp(-x)}{x^2}dx; \quad x = \frac{E_a}{RT}. \tag{4}$$

The Eq. 3 can be applied when the form of the function $p(x)$ is known.

When studying kinetics of solid-state reactions two different approaches: "model-fitting approach" and "model-free approach" are in use.

The model-fitting approach attempts to determine all three members of the kinetic triplet simultaneously from one experiment by fitting experimental data for different conversion functions [36]. In this sense, a single non-isothermal experiment provides information on $k(T)$ and $f(\alpha)$ but in an un-separated form. This is why in non-isothermal experiments almost any $f(\alpha)$ can satisfactorily fit data at the cost of dramatic variations in the Arrhenius parameters which compensate for the difference between assumed and true, but unknown, conversion function [37].

The model-free approach, also known as "isoconversion method", requires determination of the temperature T_α at which an equivalent stage of the reaction occurs for various heating rates [38]. Two widely accepted procedures are

Kissinger–Akahira–Sunose's (KAS) method [39, 40] in the form:

$$\ln\left(\frac{\beta}{T_{\alpha}^{2}}\right) = \ln\left(\frac{ZR}{E_{a,\alpha}}f(\alpha)\right) - \frac{E_{a,\alpha}}{RT_{\alpha}} \quad (5)$$

as well as the Flynn–Wall–Ozawa's (FWO) method [41, 42] in the form:

$$\ln\beta = \ln\left(\frac{ZE_{a,\alpha}}{Rg(\alpha)}\right) - 1.0518\frac{E_{a,\alpha}}{RT_{\alpha}} \quad (6)$$

where $f(\alpha)$ is the conversion function and $g(\alpha)$ is its integral form $g(\alpha) = \int \frac{d\alpha}{f(\alpha)}$.

The relations given by Eqs. 5 and 6 involve all three members of kinetic triplet. From these relations the apparent activation energy can be evaluated using the linear regression method for every value of α even when the conversion function is unknown.

Results and discussion

DTA and TG curves of $[Co(N\text{-Boc-gly})_2(H_2O)_4]\cdot 2H_2O$ complex at different heating rates ($\beta = 5$, 10, 15 and 20 °C min^{-1}) under nitrogen atmosphere in the temperature interval of 20–650 °C are shown in Fig. 1. These results show that the complex is stable up to approximately 30 °C, when the process of multi-step degradation begins. According to our previous results [17], for $\beta = 5$ °C min^{-1}, the degradation of complex starts with the dehydration of the complex. In this step, the complex losses one water molecule from the outer sphere (small peak on DTA curve in the region 30–50 °C with the rate maximum at 36.9 °C). This process is followed by immediate loss of remaining five water molecules, one from the outer and four from the inner sphere of the complex, in temperature range from 60 to 131 °C (rate maximum at 65.3 °C). After dehydration (step 1), further degradation of dehydrated complex occurs by loss of ligand fragments in two steps. The degradation of dehydrated complex happens in temperature range 131–285 °C (rate maximum at 186.2 °C). In this step, the dehydrated complex loses two identical $C_6H_5CH_2O$– ligand fragments, and then, in temperature range 285–525 °C (rate maximum at 414.0 °C) another two identical –C(=O)NHCH$_2$– ligand fragments. The result of the described thermal degradation of the complex is formation of metallic cobalt as the final product. However, for higher heating rates, Fig. 1, the dehydration shows only one well-defined endothermic peak at DTA curve; therefore the overall degradation of the complex involving the dehydration and ligand degradation, can be considered as occurring in three well separated steps.

Positions of DTA peaks, as well as corresponding mass losses on TG curves, are shifted towards higher temperatures with an increase in the heating rate, demonstrating thermal activation of all observed degradation steps [39, 42]. Intervals between peaks increase with the increasing heating rate as the activation energies of different degradation steps are different.

Well-defined TG curves with three well separated steps, Fig. 1, were used for detailed study of degradation kinetics of Co-complex between 30 and 525 °C. The mass fraction (conversion degree of reaction, α, at any temperature was determined from the ratio $\alpha = (m_o - m)/(m_o - m_f)$, where m_o is the starting mass, m is the mass at a given temperature, and m_f is the final mass of complex.

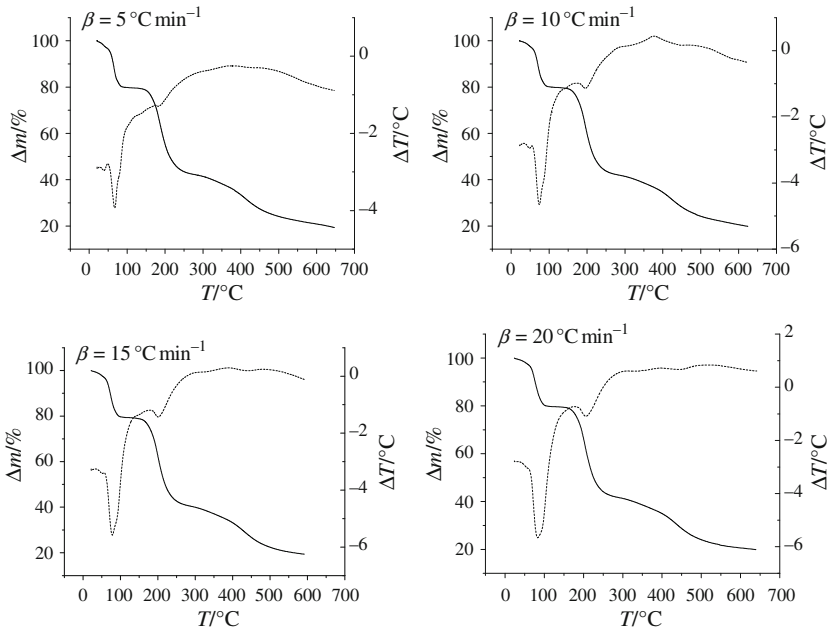

Fig. 1 TG (*solid line*) and DTA (*dashed line*) curves of $[Co(N\text{-Boc-gly})_2(H_2O)_4]\cdot 2H_2O$ complex at different heating rates in nitrogen

Model-fitting approach

In order to apply model-fitting method on the degradation process of the complex, the dependences of α versus T at different heating rates for all three observed steps are plotted, Fig. 2. The sigmoid-shaped curves are shifted to a higher temperature with an increase of heating rate, verifying that thermal activation steps are occurring during degradation.

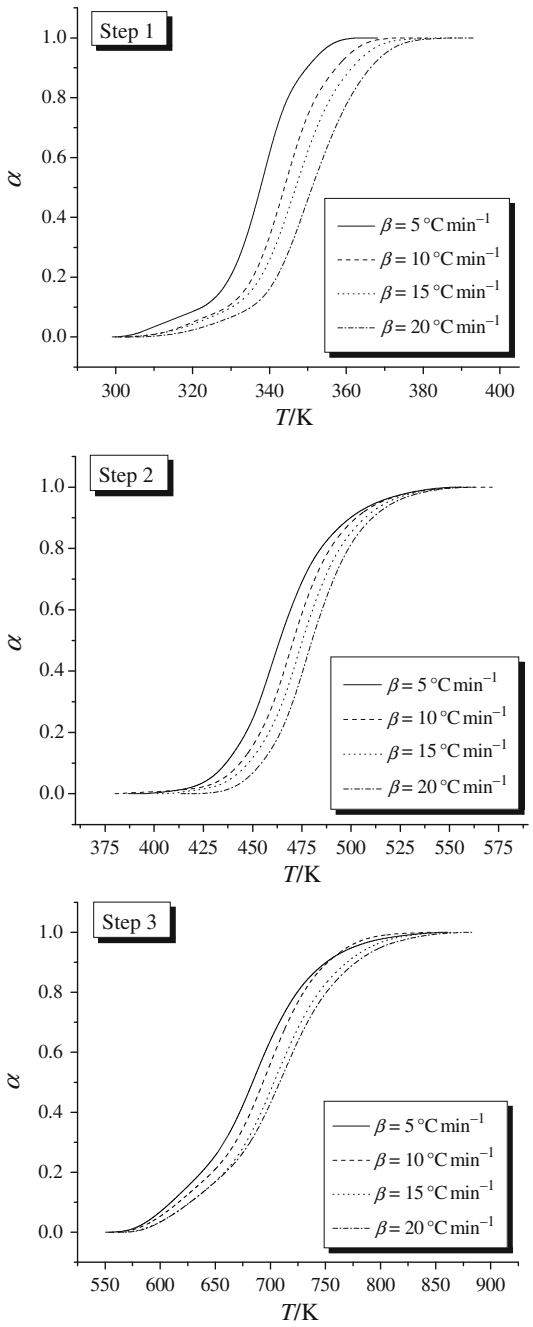

Fig. 2 Conversion degree versus temperature, for individual degradation steps at different heating rates

In order to obtain the kinetic parameters for each degradation step, the α versus T data were modelled by different conversion functions [36]. The Arrhenius parameters for every conversion function and for each heating rate were evaluated by applying Coats–Redfern method [43] (Table 1).

As can be seen from data in Table 1, although all correlation coefficients are very close to 1, the Arrhenius parameters for applied heating rates are highly variable exhibiting a strong dependence on the selected conversion function. This means that, under non-isothermal conditions, $\alpha = f(T)$ curves and Coats–Redfern's method do not permit to determine the true kinetic parameters as well as the true conversion functions. This is due to the fact that kinetic curves contain information about the temperature and conversion components in non-separated form.

Having determined the values of apparent activation energies, the conversion function for all three steps of the degradation and theoretically proposed conversion functions [36], were reconstructed numerically by applying the "master plot" method [44]. According to this method, for a single-step process, the following equation is easily derived from Eq. 1 by using a reference point at $\alpha = 0.5$

$$\frac{\mathrm{d}\alpha/\mathrm{d}t \quad \exp(E_a/RT)}{(\mathrm{d}\alpha/\mathrm{d}t)_{\alpha=0.5}\exp(E_a/RT_{0.5})} = \frac{f(\alpha)}{f(0.5)} \tag{7}$$

where $f(0.5)$ is a constant for given conversion function.

Equation 7 means that, for selected α, the experimentally determined value of the reduced-generalized reaction rate in the form

$$\frac{\mathrm{d}\alpha/\mathrm{d}t \quad \exp(E_a/RT)}{(\mathrm{d}\alpha/\mathrm{d}t)_{\alpha=0.5}\exp(E_a/RT_{0.5})}$$

and theoretically calculated value of $\frac{f(\alpha)}{f(0.5)}$ are equal when an appropriate conversion function, $f(\alpha)$, is applied. Figure 3 shows theoretical master plots of $f(\alpha)/f(0.5)$ versus α, assuming various $f(\alpha)$ functions, together with experimental plots

$$\frac{\mathrm{d}\alpha/\mathrm{d}t \quad \exp(E_a/RT)}{(\mathrm{d}\alpha/\mathrm{d}t)_{\alpha=0.5}\exp(E_a/RT_{0.5})}.$$

As can be seen from Fig. 3, the experimental data do not fit any tested model. This indicates that the analyzed steps (dehydration as well as further degradation) are not single-step reactions that could be described by conversion functions from Table 1.

Model-free approach: evaluation of the reaction mechanism

Just like in our case, most solid-state reactions are not simple one-step processes, but involve a combination of

Table 1 Apparent activation parameters, according to the Coats–Redfern equation for all used conversion functions at different heating rates

Conversion function	$\beta = 5$/°C min^{-1}			$\beta = 10$/°C min^{-1}			$\beta = 15$/°C min^{-1}			$\beta = 20$/°C min^{-1}		
j	ln Z_β/ min^{-1}	E_β/ kJ mol^{-1}	*r*	ln Z_β/ min^{-1}	E_β/ kJ mol^{-1}	*r*	lnZ_β/ min^{-1}	E_β/ kJ mol^{-1}	*r*	ln Z_β/ min^{-1}	E_β/ kJ mol^{-1}	*r*
Step 1												
P4	4.2	18.8	0.994	4.6	18.5	0.995	4.0	16.3	0.995	4.5	16.8	0.987
P3	7.4	27.0	0.995	7.7	26.5	0.996	6.9	23.6	0.996	7.4	24.4	0.989
P2	13.5	43.2	0.995	13.7	42.6	0.996	12.3	38.2	0.996	12.9	39.5	0.991
P3/2	48.8	140.9	0.996	47.8	139.0	0.997	43.2	126.0	0.997	44.3	129.9	0.993
A3/2	26.8	78.5	0.998	23.1	68.0	0.994	24.3	70.8	0.999	22.2	65.0	0.995
A2	19.1	57.5	0.998	16.4	49.6	0.994	17.5	51.7	0.999	15.9	47.3	0.994
A3	11.2	36.4	0.998	9.6	31.1	0.993	10.4	32.5	0.999	9.4	29.6	0.994
A4	7.1	25.9	0.998	6.1	21.9	0.992	6.8	23.0	0.999	6.1	20.7	0.993
B1	52.7	151.6	0.955	48.9	141.9	0.962	46.7	135.8	0.967	47.1	137.9	0.974
R1	31.3	92.0	0.996	30.9	90.8	0.997	27.9	82.1	0.997	28.8	84.7	0.992
R2	36.5	107.6	0.999	34.4	101.8	0.998	31.0	92.1	0.999	32.0	95.2	0.996
R3	35.8	106.7	0.996	35.5	105.8	0.999	31.9	95.7	0.999	32.9	99.0	0.997
D1	66.1	189.7	0.996	64.6	187.2	0.997	54.1	158.1	0.991	59.7	175.1	0.993
D2	72.7	209.2	0.998	69.1	201.2	0.998	62.3	182.6	0.998	63.9	188.4	0.995
D3	79.7	232.1	0.999	73.5	217.2	0.999	63.5	189.6	0.997	67.9	203.8	0.997
D4	74.0	216.8	0.998	69.6	206.5	0.998	59.3	178.1	0.995	64.2	193.5	0.996
F1	37.1	106.8	0.995	36.3	104.8	0.994	33.2	96.0	0.996	33.6	97.6	0.995
Step 2												
P4	0.2	14.1	0.973	1.3	15.5	0.981	1.6	15.4	0.982	2.3	17.0	0.976
P3	2.5	21.4	0.979	3.6	23.2	0.985	3.9	23.1	0.986	4.7	25.3	0.981
P2	6.6	35.8	0.983	7.9	38.7	0.988	8.2	38.6	0.988	9.3	41.9	0.984
P3/2	29.6	122.6	0.987	32.1	131.3	0.991	32.1	131.2	0.991	34.7	141.5	0.988
A3/2	14.8	64.8	0.997	16.5	69.5	0.998	14.7	62.0	0.994	15.8	65.6	0.992
A2	9.9	46.7	0.996	11.3	50.2	0.998	10.0	44.5	0.993	10.9	47.2	0.991
A3	4.7	28.6	0.995	6.0	30.9	0.998	5.2	27.0	0.991	5.9	28.8	0.989
A4	2.1	19.6	0.994	3.2	21.2	0.997	2.6	18.3	0.989	3.2	19.6	0.987
B1	22.2	94.7	0.953	26.7	110.3	0.957	27.9	114.7	0.959	29.8	122.3	0.962
R1	18.3	79.2	0.986	20.2	85.0	0.990	20.3	84.9	0.991	22.1	91.7	0.987
R2	20.5	89.5	0.993	22.6	95.9	0.995	22.7	95.8	0.996	24.7	103.5	0.993
R3	21.2	93.2	0.994	23.2	99.8	0.997	23.4	99.7	0.997	25.4	107.7	0.995
D1	40.7	166.0	0.988	43.8	177.7	0.991	43.7	177.6	0.991	47.1	191.3	0.988
D2	43.7	179.0	0.991	47.0	191.4	0.994	46.8	191.3	0.994	50.4	206.1	0.992
D3	46.4	194.0	0.995	49.8	207.3	0.997	49.6	207.1	0.997	53.5	223.3	0.995
D4	43.6	184.0	0.993	46.9	196.7	0.995	46.8	196.5	0.995	50.4	211.8	0.993
F1	24.5	101.0	0.997	23.5	96.3	0.994	23.8	97.0	0.994	25.3	102.4	0.993
Step 3												
P4	−3.6	7.1	0.983	−2.9	7.2	0.995	−2.5	7.5	0.990	−2.5	6.5	0.991
P3	−2.0	13.1	0.991	−1.3	13.3	0.998	−0.9	13.8	0.995	0.9	12.4	0.996
P2	0.6	25.1	0.995	1.3	25.5	0.999	1.8	26.3	0.997	1.6	24.3	0.998
P3/2	13.9	97.0	0.997	14.6	98.5	0.999	15.2	101.3	0.998	14.3	95.3	0.999
A3/2	5.4	48.2	0.997	6.2	49.0	0.998	6.3	48.6	0.997	6.7	49.3	0.999
A2	2.5	33.4	0.997	3.2	33.9	0.998	3.4	33.6	0.997	3.8	34.1	0.998
A3	−0.8	17.5	0.992	0.1	18.9	0.997	0.3	18.5	0.995	0.7	18.8	0.997

Table 1 continued

Conversion function j	$\beta = 5$/°C min^{-1}			$\beta = 10$/°C min^{-1}			$\beta = 15$/°C min^{-1}			$\beta = 20$/°C min^{-1}		
	ln Z_β/ min^{-1}	E_β/ kJ mol^{-1}	r	ln Z_β/ min^{-1}	E_β/ kJ mol^{-1}	r	lnZ_β/ min^{-1}	E_β/ kJ mol^{-1}	r	ln Z_β/ min^{-1}	E_β/ kJ mol^{-1}	r
A4	−2.4	11.2	0.994	−1.4	12.5	0.997	−1.1	12.4	0.996	0.7	18.8	0.997
B1	17.3	115.4	0.962	21.8	138.4	0.968	19.3	124.1	0.964	−1.1	11.2	0.996
R1	7.4	61.0	0.997	8.2	62.0	0.999	8.7	63.8	0.998	18.7	119.6	0.963

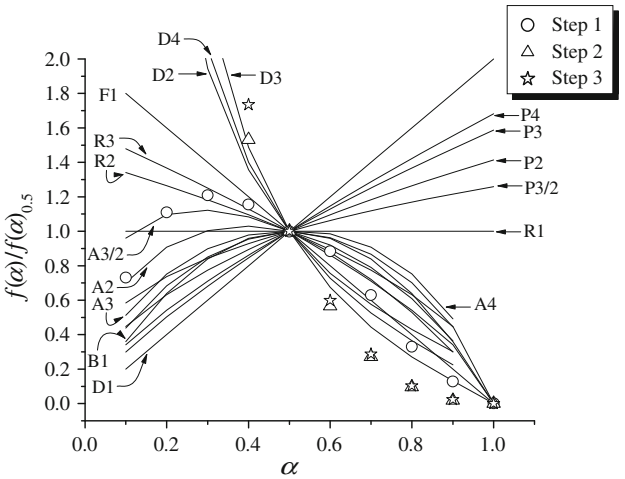

Fig. 3 Theoretical (*lines*) and calculated (*symbols*) master curves in differential form representing $f(\alpha)/f(0.5)$ as a function of α for different conversion functions describing solid-state reactions

serial and parallel elementary steps resulting in the activation energy that changes during the reaction; therefore both Arrhenius parameters should be functions of the conversion degree. Problems caused by a complex nature of degradation steps could be solved by application of "the model-free approach" [39–42].

According to this approach, the linear isoconversional relationships of $\ln\left(\beta/T_\alpha^2\right)$ versus $1/T_\alpha$ and $\ln\,\beta$ versus $1/T_\alpha$, describing non-isothermal TG data for different heating rates, can be used to determine the kinetic parameters: apparent activation energies $E_{a,\alpha}$ and intercepts $\ln\left[ZRf(\alpha)/E_{a,\alpha}\right]$ or $\ln\left[ZE_{a,\alpha}/Rg(\alpha)\right]$ for selected conversion degree, from Eqs. 5 and 6, respectively, without the knowledge of the true conversion function. The calculated values of the apparent activation energies, E_a, and intercepts as a function of the conversion degree are shown in Figs. 4, 5 and 6. The values of kinetic parameters determined by both methods are in agreement within the limits of experimental error. Very similar shape of corresponding curves for each step suggests that the apparent activation energy and intercept have a similar dependence on the conversion degree. Once again, changes of the activation energies and intercepts with conversion degree indicate complex processes involving more than one step. On the

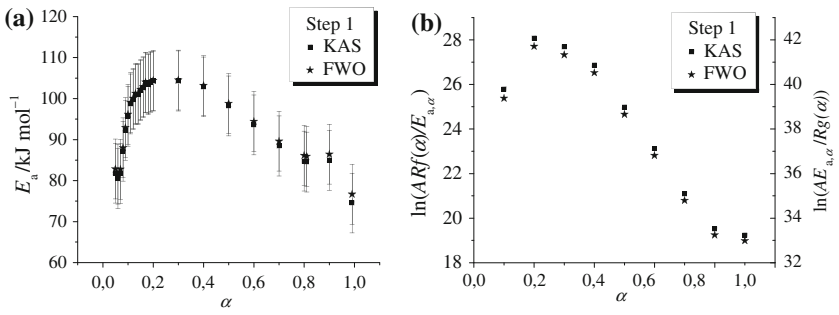

Fig. 4 **a** The apparent activation energy (bars represent standard deviation of 7.3 kJ mol^{-1}) and **b** the intercept as a function of conversion degree determined by KAS and FWO methods for step 1

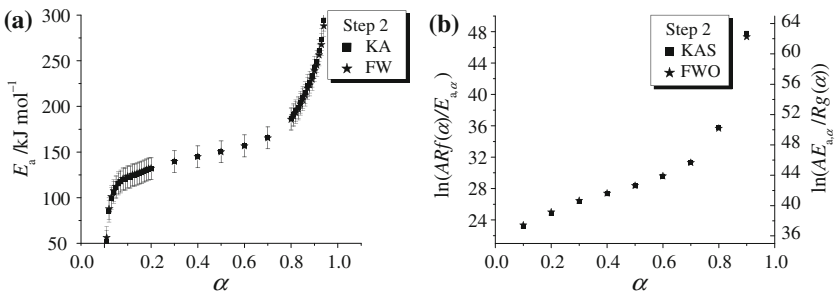

Fig. 5 **a** The apparent activation energies (bars represent standard deviation of 12.0 kJ mol^{-1}) and **b** intercept as a function of conversion degree determined by KAS and FWO methods for step 2

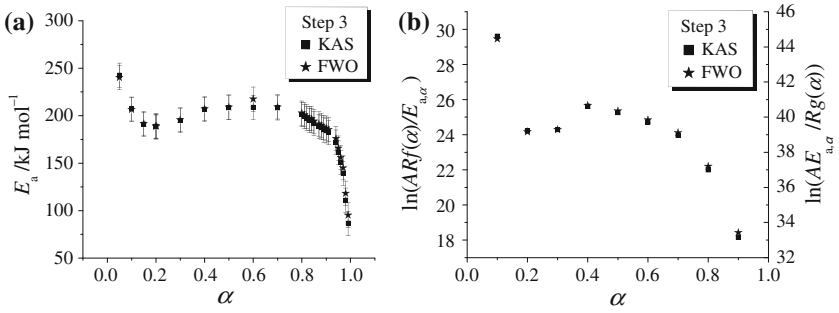

Fig. 6 **a** The apparent activation energies (bars represent standard deviation of 12.7 kJ mol^{-1}) and **b** intercept as a function of conversion degree determined by KAS and FWO methods for step 3

other hand, when curves for all three steps are compared to each other, their different shapes (Figs. 4, 5 and 6) indicates a different mechanism, which is expected taking into account the structure of the complex and the nature of the degradation fragments [33]. In the case of complex processes involving the parallel reactions, as we have here, the isoconversional methods give the activation energy that reflect kinetics of entire process [34, 45]. At the beginning ($\alpha = 0.1$) where the first reaction is predominant, the obtained activation energy corresponds to the value of first reaction. Contrary, at the end of the process ($\alpha = 0.9$) where the second reaction prevails, the obtained activation energy correspond to second reaction.

For dehydration of the complex, step 1, an increase and then decrease of E_a as the reaction proceeds is observed, Fig. 4a. In this case, the $E_{a,\alpha}$ increases from 81.8 kJ mol^{-1}, for $\alpha = 0.05$, reaching the maximum of 104.3 kJ mol^{-1} at $\alpha = 0.3$, and then decreases to 74.5 kJ mol^{-1} at $\alpha = 1.0$. The observed convex shape of the function $E_a = f(\alpha)$ indicates a complex process of dehydration of the complex [16]. According to the algorithm described in Ref. [46], and formula of the complex [Co(*N*-Boc-gly)$_2$(H$_2$O)$_4$]·2H$_2$O dehydration involves a series of competitive dehydration steps of differently bound water molecules [16] complicated by diffusion [33].

For degradation of dehydrated complex, step 2 (Fig. 5a), the $E_{a,\alpha}$ increases during the entire process, but at different rates. In the beginning, the activation energy is 52.2 kJ mol^{-1}. It increases quickly, reaching about 130 kJ mol^{-1} at $\alpha = 0.2$, continues to increase slowly up to $\alpha = 0.7$ and finally rises sharply to 243 kJ mol^{-1} at $\alpha = 0.9$. This indicates a complex mechanism involving parallel reactions [46]. In this step, the dehydrated complex losses two identical $C_6H_5CH_2O$– ligand fragments. The products in gaseous state increase the overall pressure in the reaction system, as can be expected for reaction solid = solid + gas [47]. So, an increase in pressure enhances the reverse reaction, which shifts the overall process of decomposition to higher temperatures, resulting in an observed increase of the apparent activation energy.

In the next degradation step (step 3), the dependence of activation energy on conversion degree, Fig. 6a, shows an overall drop. At the beginning, the activation energy decreases from 242.6 kJ mol^{-1} ($\alpha = 0.05$) to 188 kJ mol^{-1} ($\alpha = 0.2$), then fluctuates between 192 and 209 kJ mol^{-1}, and finally, starting from $\alpha = 0.9$, drops to 86.7 kJ mol^{-1}. The decreasing trend with the change from concave to convex shape of the curve (Fig. 6a) indicates a complex process with a change in the limiting stage. In this case that could be the change from kinetic to diffusion regime connected with the presence of gaseous products diffusing through the solid product [46].

Evaluation of kinetics parameters and isokinetic relationships

Although isoconversional or model-free methods offer an opportunity to establish the dependency of energy activation on conversion degree as well as the mechanism of reaction, they do not give any information about the other two members, Z and $f(\alpha)$, of the kinetic triplet. Therefore, based on the conclusion that all three steps of degradation are complex, the results of isoconversional methods (KAS and FWO) are further combined with a model-independent estimation of the pre-exponential factor using an artificial (false) isokinetic relationship (IKR) [48].

Generally speaking, IKR is based on a common point of intersection of Arrhenius lines [33]:

$$\ln Z = \ln k_{\text{iso}} + \frac{E}{R\left(T_{\text{iso}}^{-1} - T^{-1}\right)}$$

where k_{iso} is the isokinetic rate constant and T_{iso} is the isokinetic temperature, and on a linear correlation:

$$\ln Z_\xi = a + bE_\xi \tag{8}$$

where $a = \ln k_{\text{iso}}$ and $b = 1/RT_{\text{iso}}$, also known as "compensation parameters", are coordinates of the intersection of point of Arrhenius lines. The subscript ξ refers to a factor that produces a change in Arrhenius parameters. The

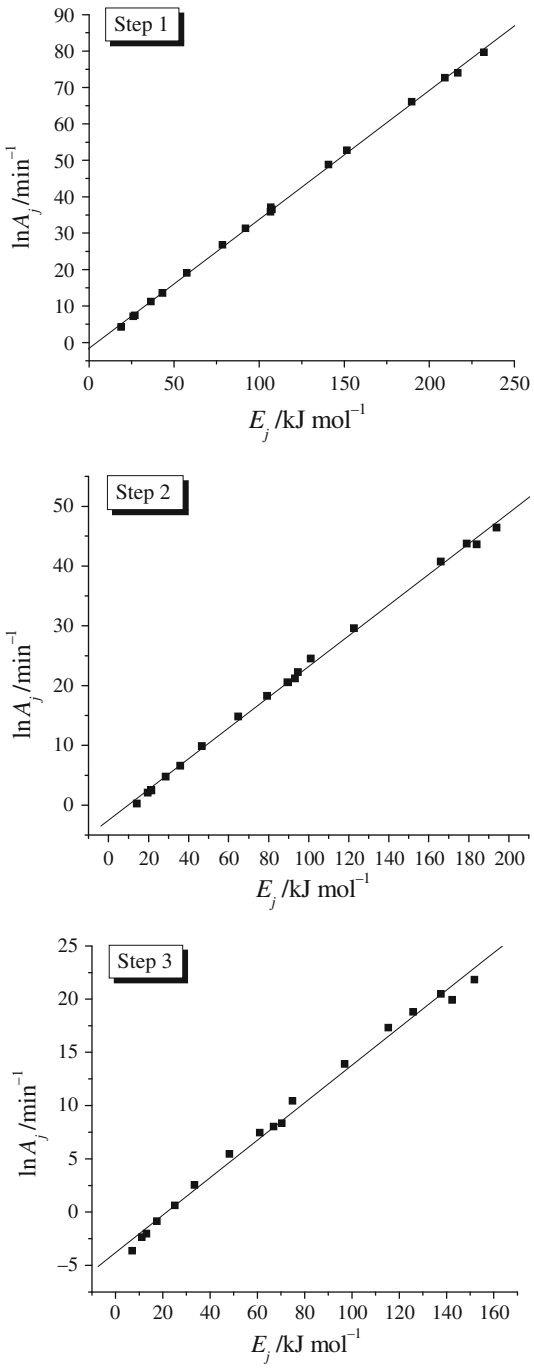

Fig. 7 The dependences $\ln A_j$ versus E_j for individual steps of degradation at heating rate 5 °C min^{-1}

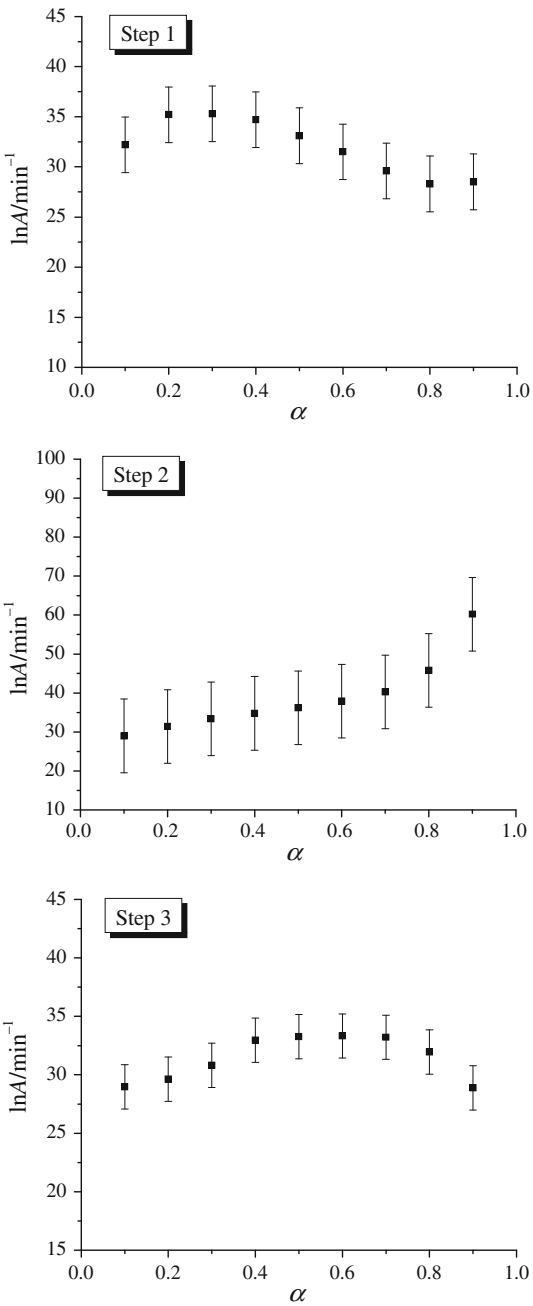

Fig. 8 The dependence $\ln A_\alpha$ versus α for all three steps of degradation. (The values of E_α determined by KAS method are used)

Arrhenius lines resulting from the model-fitting method, Table 1, intersect at one point indicating that Arrhenius parameters related to different reaction models will show a linear correlation

$$\ln Z_j = c + dE_j \tag{9}$$

where a subscript j denotes a reaction model.

In Fig. 7 Arrhenius parameters, ln Z_j, determined according to the relation (9) for different conversion functions j from Table 1 at heating rate 5 °C min^{-1}, is presented as an example. The obtained the linear dependences indicate the existence of the false compensation effect as it defined by (9). Having determined the compensation parameters c and d, the E_α values are substituted for E_j in Eq. 9 to estimate the corresponding ln Z_α, Fig. 8. A similarity with curves shown in Figs. 4, 5 and 6 is evident confirming the validity of the above assumed mechanisms.

Conclusions

Thermal degradation of $[Co(N\text{-Boc-gly})_2(H_2O)_4]\cdot 2H_2O$ is a stepwise process involving one step of dehydration and two steps of degradation of dehydrated complex. The transformations in each step cause changes in the structure and chemical composition of investigated compound, affecting the course of further degradation. In this case, all three steps of thermal degradation, involving loss of differently bounded water molecules (four in the internal and two in the external sphere of the complex) and loss of different fragments of the ligands, can be described using completely different reaction paths, affecting the shape of the dependence of Arrhenius and isokinetic parameters on conversion degree. These dependences show that all the observed steps of thermal degradation of the investigated compound are complex, involving more than one single step, as can be expected for solid-state heterogeneous reactions with solid reactants and a mixture of solid and gaseous products. Combination of model-fitting and model-free approaches in non-isothermal experiments allowed us to determine the Arrhenius parameters as well as isokinetic parameters for different conversion degrees. These results suggest the complex structure of each degradation step. However, the complex nature of each step precludes the determination of the corresponding conversion functions, but, using the algorithm developed for complex solid reactions based on the dependence of Arrhenius parameters on conversion degree, we could propose the mechanism for each of the observed steps. This study shows that the criteria suggested by Vyazovkin for polymeric, simple inorganic solids and glass materials [32, 33, 37, 46], could also be applied to very complex processes of degradation of coordination compounds and allows determination of the mechanism and kinetics of degradation. This will be the subject of our future studies on another coordination compounds as model systems.

Acknowledgements This work was supported by the Ministry of Science and Technological Development of the Republic of Serbia, Grant Nos. 172015, 172055 and 45007.

References

1. Sreenivasulu B. Diphenoxo-bridged copper(II) complexes of reduced schiff base ligands as functional models for catechol oxidase. Aust J Chem. 2009;62:968–79.
2. Kadyrov MA, Mutalibov AS. Synthesis and study of mono- and dinuclear cobalt(II) complexes with *N*-substituted pyridoxalidene derivatives of α-amino acids. O'zb Kim J. 2003;3:16–21.
3. Perez-Cadenas A, Godino-Salido L, Lopez-Garzon R, Arranz-Mascaros P, Gutierrez-Valero D, Cuesta-Martos R. The reactivity of N-2-(4-amino-1,6-dihydro-1-methyl-5-nitroso-6-oxopyrimidinyl)-L-histidine towards copper(II) ions. Transition Met Chem. 2001; 26:581–7.
4. Saladini M, Iacopino D, Menabue L. Metal(II) binding ability of a novel N-protected amino acid. A solution-state investigation on binary and ternary complexes with 2,2'-bipyridine. J Inorg Biochem. 2000;78:355–61.
5. Godino Salido ML, Arranz Mascaros P, Lopez Garzon R, Gutierrez Valero MD, Low JN, Gallagher JF, Glidewell C. Hydrated metal(II) complexes of N-(6-amino-3,4-dihydro-3-methyl-5-nitroso-4-oxopyrimidin-2-yl) derivatives of glycine, glycylglycine, threonine, serine, valine and methionine: a monomeric complex and coordination polymers in one, two and three dimensions linked by hydrogen bonding. Acta Crystallogr B. 2004;60:46–64.
6. Herrick RS, Dupont J, Wrona I, Pilloni J, Beaver M, Benotti M, Powers F, Ziegler CJ. Preparation and characterization of d6 tungsten compounds with amino acid derivatized diimine ligands and preparation of dipeptide derivatives using peptide coupling agents. J Organomet Chem. 2007;692:1226–33.
7. Jiang T, Zhang Z, Wan S. Preparation of benzisoselenazolone aminosugar derivative as antitumor agent. Faming Zhuanli Shenqing Gongkai Shuomingshu. 2007;A:CN 101016319.
8. Baxter AD, Montana J, Owen DA. Preparation and therapeutic use of sulfhydryl and acylthio peptide amides as matrix metalloproteinase and tumor necrosis factor inhibitors. PCT Int Appl. 1996;A1:WO 9635687.
9. Pinel AM. Preparation of novel peptide derivatives and their therapeutic and cosmetic application. PCT Int Appl. 2003;A2: WO 2003064458.
10. Lambert DM, Geurts M, Scriba GKE, Poupaert JH, Dumont P. Simple derivatives of amino acid neurotransmitters. Anticonvulsant evaluation of derived amides, carbamates and esters of glycine and beta-alanine. J Pharm Belg. 1995;50:194–203.
11. Nomiya K, Takahashi S, Noguchi R, Nemoto S, Takayama T, Oda M. Synthesis and characterization of water-soluble silver(I) complexes with L-histidine (H2his) and (S)-(−)-2-pyrrolidone-5-carboxylic acid (H2pyrrld) showing a wide spectrum of effective antibacterial and antifungal activities. Crystal structures of chiral helical polymers [Ag(Hhis)]n and {[Ag(Hpyrrld)]2}n in the solid state. Inorg Chem. 2000;39:3301–11.
12. Nomiya K, Takahashi S, Noguchi R. Water-soluble silver(I) complexes of (*R*)-(+)- and (*S*)-(−)-2-pyrrolidone-5-carboxylic acid and their antimicrobial activities. Chiral helical polymer and polymer sheet structures in the solid-state formed by self-assembly of dimeric $[Ag(Hpyrrld)]_2$ cores. J Chem Soc Dalton Trans. 2000; 4369–73.
13. Nomiya K, Takahashi S, Noguchi R. Synthesis and crystal structure of three silver(I) complexes with (*S*)-(+)-5-oxo-2-tetrahydrofurancarboxylic acid (S-Hothf) and its isomeric forms (R-Hothf and R,S-Hothf) showing wide spectra of effective antibacterial and antifungal activities. Chiral helical polymers in the solid state formed by self-assembly of the dimeric $[Ag(othf)]_2$ cores. J Chem Soc Dalton Trans. 2000;1343-8.
14. Chikaraishi Kasuga NC, Yamamoto R, Hara A, Amano A, Nomiya K. Molecular design, crystal structure, antimicrobial activity and reactivity of light-stable and water-soluble Ag–O bonding silver(I) complexes, dinuclear silver(I) *N*-acetylglycinate. Inorg Chim Acta. 2006;359:4412–6.
15. Mitić D, Milenković M, Milosavljević S, Gođevac D, Miodragović Z, Anđelković K, Miodragović Đ. Synthesis, characterization and antimicrobial activity of Co(II), Zn(II) and Cd(II) complexes with *N*-benzyloxycarbonyl-*S*-phenylalanine. Eur J Med Chem. 2009;44:1537–44.
16. Miodragović ĐU, Mitić DM, Miodragović ZM, Bogdanović GA, Vitnik ŽJ, Vitorović MD, Radulović MĐ, Nastasijević BJ, Juranić IO, Anđelković KK. Syntheses, characterization and antimicrobial activity of the first complexes of Zn(II), Cd(II) and Co(II) with *N*-benzyloxycarbonylglycine: X-ray crystal structure

of the polymeric Cd(II) complex. Inorg Chim Acta. 2008;361: 86–94.
17. Šumar-Ristović MT, Minić DM, Poleti D, Miodragović Z, Miodragović Đ, Anđelković KK. Thermal stability and degradation of Co(II), Cd(II), and Zn(II) complexes with *N*-benzyloxycarbonylglycinato ligand. J Thermal Anal Calorim. 2010;102: 83–90.
18. Ababei LV, Kriza A, Musuc AM, Andronescu C, Rogozea EA. Thermal behaviour and spectroscopic studies of complexes of some divalent transitional metals with 2-benzoil-pyridilizonicotinoylhydrazone. J Therm Anal Calorim. 2010;101:987–96.
19. Asadi M, Ghatee MH, Torabi S, Mohammadi K, Moosavi F. Synthesis, characterization, ab initio calculations, thermal behaviour and thermodynamics of some oxovanadium(IV) complexes involving O, O- and N, N-donor moieties. J Chem Sci. 2010;122(4):539–48.
20. Khalil MMH, Ismail EH, Azim SA, Souaya ER. Synthesis, characterization, and thermal analysis of ternary complexes of nitrilotriacetic acid and alanine or phenylalanine with some transition metals. J Therm Anal Calorim. 2010;101:129–35.
21. Serebryanskaya TV, Ivashkevich LS, Lyakhov AS, Gaponik PN, Ivashkevich OA. 1,3-Bis(2-alkyltetrazol-5-yl)triazenes and their Fe(II), Co(II) and Ni(II) complexes: synthesis, spectroscopy, and thermal properties. Crystal structure of Fe(II) and Co(II) 1, 3-bis(2-methyltetrazol-5-yl)triazenide complexes. Polyhedron. 2010;29:2844–50.
22. Doğan F, Dayan O, Yürekli M, Çetinkaya B. Thermal study of ruthenium(II) complexes containing pyridine-2,6-diimines. J Therm Anal Calorim. 2008;91:943–9.
23. Doğan F, Ulusoy M, Öztürk ÖF, Kaya İ, Salih B. Synthesis, characterization and thermal study of some tetradentate Schiff base transition metal complexes. J Therm Anal Calorim. 2009;98: 785–92.
24. Sun J, Lu Z, Li Y, Dai J. Thermal behaviour and decomposition kinetics for two palladium(II) complexes with 1-aminopyrene and its derivative. J Therm Anal Calorim. 1999;58:383–91.
25. Zsakó J, Pokol G, Novák Cs, Várhelyi Cs, Dobó A, Liptay G. Kinetic analysis of TG Data XXXV. Spectroscopic and thermal studies of some cobalt(III) chelates with ethylenediamine. J Therm Anal Calorim. 2001;64:843–56.
26. Bajpai A, Tiwari S. Application of thermogravimetric analysis for characterisation of bisdithiocarbamate of urea and its copper (II) complex. Thermochim Acta. 2004;411:139–48.
27. Al-Maydama H, El-Shekeil A, Khalid MA, Al-Karbouly A. Thermal degradation behaviour of some polydithiooxamide metal complexes. Eclética Quim. 2006;31:45–52.
28. Shen XQ, Li ZJ, Niu YL, Qiao HB. Crystal structure, thermal behavior, and non-isothermal kinetics of a new dinuclear Ni(II) complex. Synth React Inorg Met-Org Chem. 2009;39:55–9.
29. Kaya I, Solguntekin A. Synthesis, characterization, and kinetic of thermal degradation of oligo-2-[(4-bromophenylimino)methyl] phenol and oligomer-metal complexes. J Appl Polym Sci. 2009; 113:1994–2007.
30. Guinesi LS, Ribeiro CA, Crespi MS, Veronezi AM. (II)-EDTA complex kinetic of thermal decomposition by non-isothermal procedures. Thermochim Acta. 2004;414:35–42.
31. Budrugeac P. Some methodological problems concerning the kinetic analysis of non-isothermal data for thermal and thermooxidative degradation of polymers and polymeric materials. Polym Degrad Stab. 2005;89:265–73.
32. Vyazovkin S. A unified approach to kinetic processing of nonisothermal data. Int J Chem Kinet. 1996;28:95–101.
33. Vyazovkin S, Wight CA. Kinetics in solids. Annu Rev Phys Chem. 1997;48:125–49.
34. Vyazovkin S, Linert W. Detecting isokinetic relationships in nonisothermal systems by the isoconversional method. Thermochim Acta. 1995;269(/270):61–72.
35. Brown ME, Dollimore D, Galwey AK. Reaction in the solid state: comprehensive chemical kinetics. In: Bamford CH, Tipper CFH, editors. Amsterdam: Elsevier, 1980. p. 22.
36. Dollimore D, Tong P, Alexander KS. The kinetic interpretation of the decomposition of calcium carbonate by use of relationships other than the Arrhenius equation. Thermochim Acta. 1996;282(/ 283):13–27.
37. Vyazovkin S, Wight C. Isothermal and non-isothermal kinetics of thermally stimulated reactions of solids. Int Rev Phys Chem. 1998;17:407–33.
38. Starink MJ. The determination of activation energy from linear heating rate experiments: a comparison of the accuracy of isoconversion methods. Thermochim Acta. 2003;404:163–76.
39. Kissinger HE. Reaction kinetics in differential thermal analysis. Anal Chem. 1957;29:1702–6.
40. Akahira T, Sunose T. Trans joint convention of four electrical institutes, Paper No. 246, 1969. Research Report. Chiba Institute of Technology. 1971;16:22–31.
41. Flynn JH, Wall LA. General treatment of the thermogravimetry of polymers. J Res Natl Bur Stand Sect A. 1966;70:487–523.
42. Ozawa T. A new method of analyzing thermogravimetric data. Bull Chem Soc Japan. 1965;38:1881–6.
43. Coats AW, Redfern JP. Kinetic parameters from thermogravimetric data. Nature. 1964;201:68–9.
44. Gotor FJ, Criado JM, Malek J, Koga N. Kinetic analysis of solidstate reactions: the Universality of Master Plots for analyzing isothermal and nonisothermal experiments. J Phys Chem A. 2000;104:10777–82.
45. Vyazovkin S, Linert W. The application of isoconversional methods for analyzing isokinetic relationships occurring at thermal decomposition of solids. J Solid State Chem. 1995;114: 392–8.
46. Vyazovkin S, Lesnikovich AI. An approach to the solution of the inverse kinetic problem in the case of complex processes. 1. Methods employing a series of thermoanalytical curves. Thermochim Acta. 1990;165:273–80.
47. Lyakhov NZ, Maciejewski M, Reller A. Theoretical considerations on the temperature and pressure dependence of the kinetics of reversible thermal decomposition processes of solids. J Solid State Chem. 1985;58:398–400.
48. Vyazovkin S, Linert W. Evaluation and application of isokinetic relationships: the thermal decomposition of solids under nonisothermal conditions. J Chem Inf Comput Sci. 1994;34:1273–8.